Design concept for CLT - reinforced with self-tapping screws*

Peter Mestek

Dr.-Ing., Structural Engineer

Sailer Stepan und Partner GmbH

Munich, Germany

Philipp Dietsch

Dr.-Ing., Research Associate, Academic Director

Lehrstuhl für Holzbau und Baukonstruktion, TU München

Munich, Germany

Summary

Concentrated loads on Cross Laminated Timber elements (CLT) in areas of point supports or load applications cause high local shear stresses. Inclined self-tapping screws with continuous threads have turned out to be an effective reinforcement. As neither the German design standard DIN 1052 [2] nor technical approvals cover this construction method a research project funded by the AiF [3] was conducted to gather basic information for its application. These basics include the determination of shear stresses next to concentrated loads, the interaction of compression perpendicular to the grain and rolling shear stresses as well as theoretical and experimental examinations of the load bearing behaviour of reinforced CLT-elements. This paper presents the main research results. A design concept validated by means of the test results is proposed [4].

1. Introduction

Ceilings of CLT are generally simply supported on two sides so that uniaxial load transfer is activated parallel to the lamellas of the top layers. Due to the composition of the CLT-elements, with an orthogonally alternating orientation of neighbouring board layers, the slabs are also suitable for constructions with point supports. These systems profit from the biaxial load transfer and the possibility of the prefabrication of large-scale elements.

Concentrated loading causes high shear stresses in these areas (Fig. 1). Since the rolling shear capacity of timber is considerably lower than its shear capacity parallel to the grain, shear-fracture appears in the cross layers of CLT elements. First tests within the scope of pilot projects revealed that reinforcement with inclined self-tapping screws noticeably enhance the shear capacity of the CLT-elements [5]. As this reinforcement is not covered by the current design standards, a research project funded by the AiF [3] was conducted to gather basic information for their application.

* The contents of the paper have first been presented at the CIB W18 Meeting 2011 in Alghero, Italy [1]

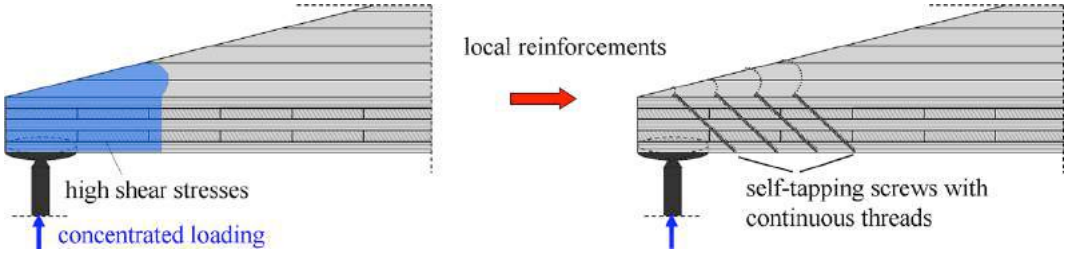

Fig. 1 Local reinforcement by self-tapping screws with continuous threads

2. Experimental tests

Within the scope of the project various experimental tests were carried out. Some small-scale tests were necessary to determine material and system parameters for the FEM-simulations carried out in parallel. Tests with CLT-elements supplied basic information for the interaction of rolling shear and compression perpendicular to the grain as well as for the load bearing behaviour and the strengthening effect of CLT-elements reinforced by self-tapping screws.

2.1 Material and fabrication

The cross section of the test specimens consisted of seven layers, the total thickness of the elements was 119 mm (7 x 17 mm) and 189 mm (7 x 27 mm). The base plates were built up of spruce boards of grade S10 (visual grading according to DIN 4074-1 [6]) that were not glued along their edges. The density of the boards for the cross layers ranged between 440 kg/m^3 and 480 kg/m^3. Due to the fabrication process by vacuum gluing, the lamellas of the test series “Type 119” and “Type 189” had relief grooves parallel to the grain as shown in Fig. 2.

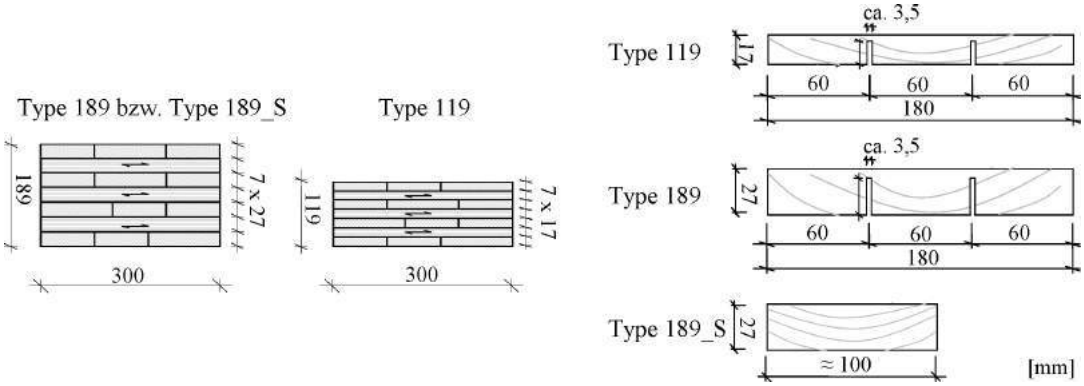

Fig. 2 Cross sections and dimensions of the single boards

2.2 Interaction of rolling shear stresses and compression perpendicular to the grain

Concentrated loading in CLT elements causes a combination of high shear stresses and compression perpendicular to the grain (Fig. 3). The positive effect of compression on the shear capacity parallel to the grain is an established fact and has been the object of various investigations [7], [8]. However, comparable evaluations concerning the interaction of rolling shear strength and compression perpendicular to the grain are not yet available. Hence experimental tests were carried out to gather first information on the increase in rolling shear capacity due to this stress interaction. Therefore shear elements inclined against the vertical by 10° were stressed by a shear force. The shear force was induced into the layers parallel to the primary direction (Fig. 4). The initiation of the compression was developed by lateral steel

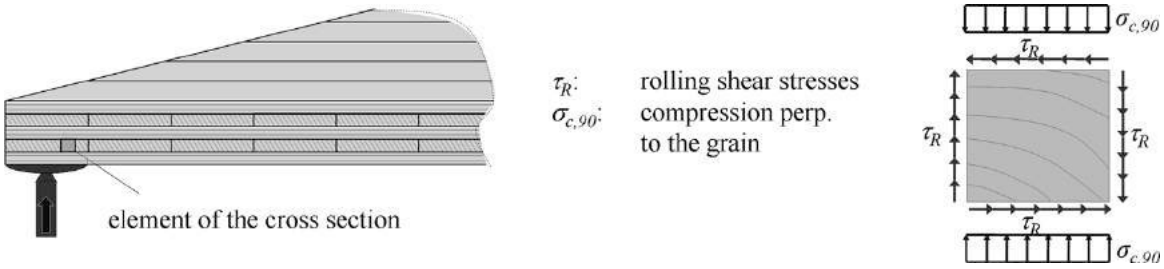

Fig. 3 Interaction of rolling shear and compression perp. to the grain caused by concentrated loading

profiles (HEA 100) coupled with exterior rods. The rods in combination with the head plates and the impression cylinder enabled the initiation of a specific compression that could be controlled by the load cell. Friction minimizing teflon plates between the test specimens and the steel profiles avoided any transfer of shear forces by the framework and guaranteed free shear deformation of the test samples. The base elements had a width of 300 mm. As shown in Fig. 4, five base elements of each section type were separated into three test specimens. To minimize the variation of the results, one test specimen per base element was assigned to each test series. In order to determine a reference value one series (i = 0) of each section type was tested without external pre-stressing.

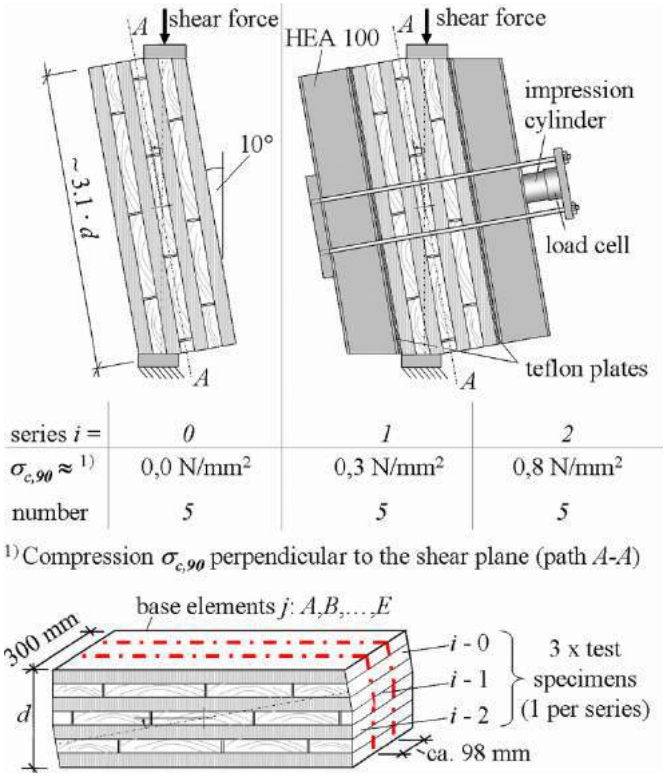

series i =	0	1	2
$\sigma_{c,90} \approx$ [1)]	0,0 N/mm²	0,3 N/mm²	0,8 N/mm²
number	5	5	5

[1)] Compression $\sigma_{c,90}$ perpendicular to the shear plane (path A-A)

Fig. 4 Test configuration

The simulation of the test configuration by using an FEM-shell-model [9] shows that due to the inclined load initiation compression perpendicular to the shear plane is mainly located in the boundary region (Fig. 5). Because of its rapid decrease it was neglected in the course of further evaluations. The force component parallel to the shear plane causes an almost constant distribution of rolling shear stresses and so the rolling shear capacity was calculated on the assumption of a constant stress distribution. The mean values in Tab. 1 indicate that not only the material but also the geometric relations of the board dimensions, particularly the arrangements of the relief grooves, influence the level of resistance. It appeared that the smaller the ratio of the distance between the gaps or relief grooves to the thickness of the layers, the smaller the rolling shear capacity.

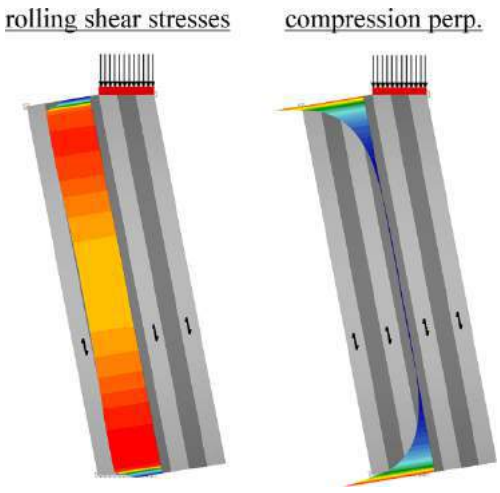

Fig. 5 Distribution of stresses

Tab. 1 Mean values of the rolling shear capacity

Elements		Type 119-*i*		Type 189-*i*		Type 189_S-*i*	
Series *i*	$\sigma_{c,90}$ [N/mm²]	$f_{R,mean,i}$ [N/mm²]	*COV* [-]	$f_{R,mean,i}$ [N/mm²]	*COV* [-]	$f_{R,mean,i}$ [N/mm²]	*COV* [-]
i = 0	0,00	1,47	0,08	0,90	0,09	1,42	0,06
i = 1	≈ 0,30	1,52	0,07	1,10	0,09	1,61	0,04
i = 2	≈ 0,80	1,84	0,07	1,27	0,06	1,83	0,04

As the reference for comparison was from tests without external pre-stressing, the main focus was directed to the increase of the strength and not on the value of the rolling shear strength itself. The increase in the rolling shear capacity can be described by the parameter, $k_{R,90}$, according to equation (1). The evaluation was carried out separately for each base element to minimize the influence of the material properties.

$$k_{R,90} = \frac{f_{R,i,j}}{f_{R,i=0,j}} \qquad \text{with} \quad i = 1, 2 \text{ and } j = A, \ldots, E \text{ (see Fig. 4)} \qquad (1)$$

The chart in Fig. 6 illustrates the evaluation of the parameter $k_{R,90}$ according to equation (1) and the corresponding regression curves of each element type. It appears that the ratio of the distance between the gaps to the thickness of the layer affects the parameter $k_{R,90}$ as well. Nevertheless it does not seem useful to consider this geometrical ratio within a practical design concept, since the influence of the ratio on the resistance is already taken into account by the characteristic rolling shear capacity in the technical approvals. In addition the design engineer generally does not know the exact dimension of the boards and even less the arrangement of the relief grooves. So, for the final proposal, the parameter $k_{R,90}$ was derived on the basis of a regression curve including all results without differentiation of the element types (Fig. 7). It represents a conservative criterion for the stress interaction that allows a maximum increase of 20 % of the rolling shear capacity. The parameter $k_{R,90}$ should be applied within the stress verification as shown in the following equations:

$$\tau_{R,d} \le k_{R,90} \cdot f_{R,d} \qquad \text{with} \quad k_{R,90} = \min \begin{cases} 1 + 0{,}35 \cdot \sigma_{c,90} \text{ [-]} \\ 1{,}20 \end{cases} \quad \text{and} \quad \sigma_{c,90} \text{ in N/mm}^2 \qquad (2) \text{ and } (3)$$

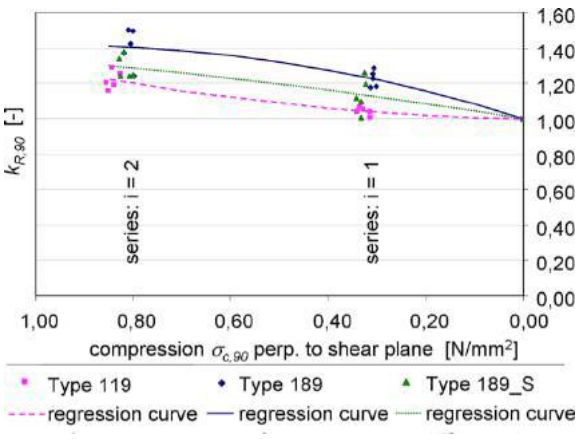

Fig. 6 Evaluation of kR,90 for each element type

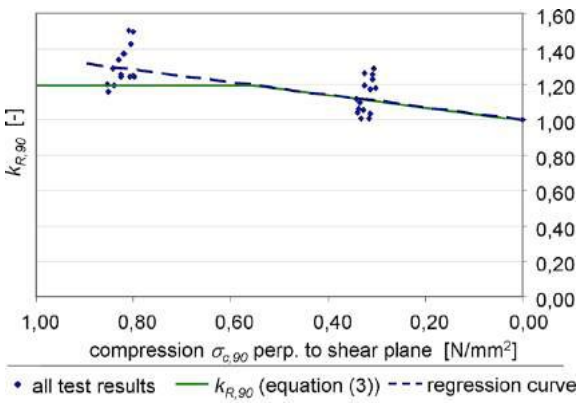

Fig. 7 Proposal for the calculation of kR,90

2.3 Reinforcement – uniaxial load transfer

The load bearing behaviour of reinforced CLT elements was analysed by means of various test configurations. Tests with shear elements that were inclined against the vertical by 10° (analogous to Fig. 4, without pre-stressing) are described and evaluated in [3]. In addition the following four-point-bending tests according to CUAP 03.04/06 [10] were carried out. The test configuration and main dimensions are shown in Fig. 8. First one unreinforced series of each element type was tested to determine a reference value of the rolling shear capacity. Tab 2 contains the calculated mean and characteristic values. Then the elements of the remaining series were reinforced with self-tapping screws with continuous threads (Spax-S [11], d = 8,0 mm).

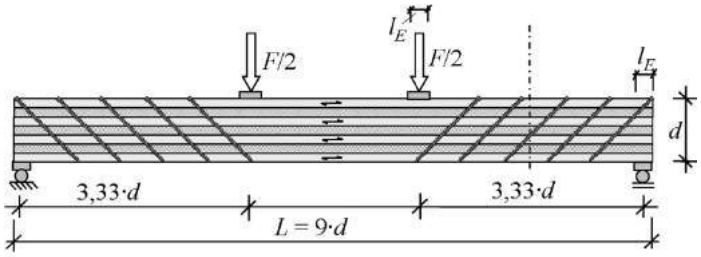

	d	L	l_E	width b	
Type 119	119	1070	50	300	[mm]
Type 189 / 189_S	189	1700	80	300	[mm]

Fig. 8 Configuration of four-point-bending tests

Tab. 2: Rolling shear capacity of the unreinforced elements

Element Type	Type 119	Type 189	Type 189_S	
$f_{R,mean,\theta}$	1,35	0,97	1,34	[N/mm²]
$f_{R,k,\theta}$	1,13	0,77	1,08	[N/mm²]
$f_{R,k}$ (acc. to abZ)	0,70	0,70	0,70	[N/mm²]

The primary criterion to describe the influence of the reinforcement on the structural behaviour is the strengthening factor $\eta_{mean,i}$. It is defined by the ratio of the proof loads of the reinforced elements to the proof loads of the unreinforced reference series:

$$\eta_{mean,i} = \frac{F_{mean,i}}{F_{mean,0}} \quad \left(= \frac{F_{mean,\ reinforced\ specimens}}{F_{mean,\ unreinforced\ specimens}} \right) \tag{4}$$

Tab. 3 to Tab. 5 give a general view of the tested arrangements of screws for each element type and also contain the strengthening factor $\eta_{mean,i}$, calculated on the basis of the test results. Each series consisted of five test specimens. The results reveal that the application of screws increases the load-carrying capacity by up to 64 %. Even comparatively few screws cause an increase of more than 25 %. So the structural behaviour is affected positively by a growing number of screws. Consequently the failure mode changes and the elements partially fail by bending and not by shear fracture.

Tab. 3: Type 119 – $\eta_{mean,i}$

Arrangement of the screws (d = 8,0 mm) in mm	Type	$\eta_{mean,i}$ [-]	COV [-]
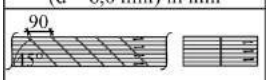	119-1	**1,25**	0,03
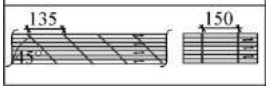	119-2	**1,30**	0,09

Tab. 4: Type 189 – $\eta_{mean,i}$

Arrangement of the screws (d = 8,0 mm) in mm	Type	$\eta_{mean,i}$ [-]	COV [-]
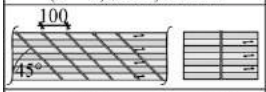	189-1	**1,31**	0,05
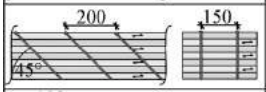	189-2	**1,38**	0,06
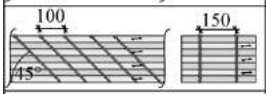	189-3	**1,64**	0,08
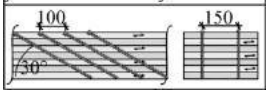	189-4	**1,59**	0,04

Tab. 5: Type 189_S – $\eta_{mean,i}$

Arrangement of the screws (d = 8,0 mm) in mm	Type	$\eta_{mean,i}$ [-]	COV [-]
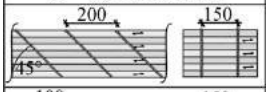	189_S-2	**1,34**	0,02
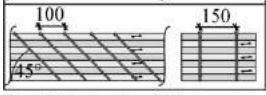	189_S-3	**1,46***	0,10*

*partially bending failure

2.4 Reinforcement – biaxial load transfer

Shear tests with plate elements were carried out to gain preliminary experience with reinforcement by self-tapping screws under biaxial load transfer. Plate elements supported along all sides and stressed by concentrated loading as well as elements with point supports in the corner regions were used according to the configurations shown in Fig. 10. A first test revealed intense indentations in the area of loading (Fig. 9). As a consequence, self-tapping screws, under the steel plates of the load application and at the point supports, were applied vertically to serve as reinforcement. Further information on this kind of reinforcement is given in [12].

Fig. 9 Intense indentations in the area of the load application

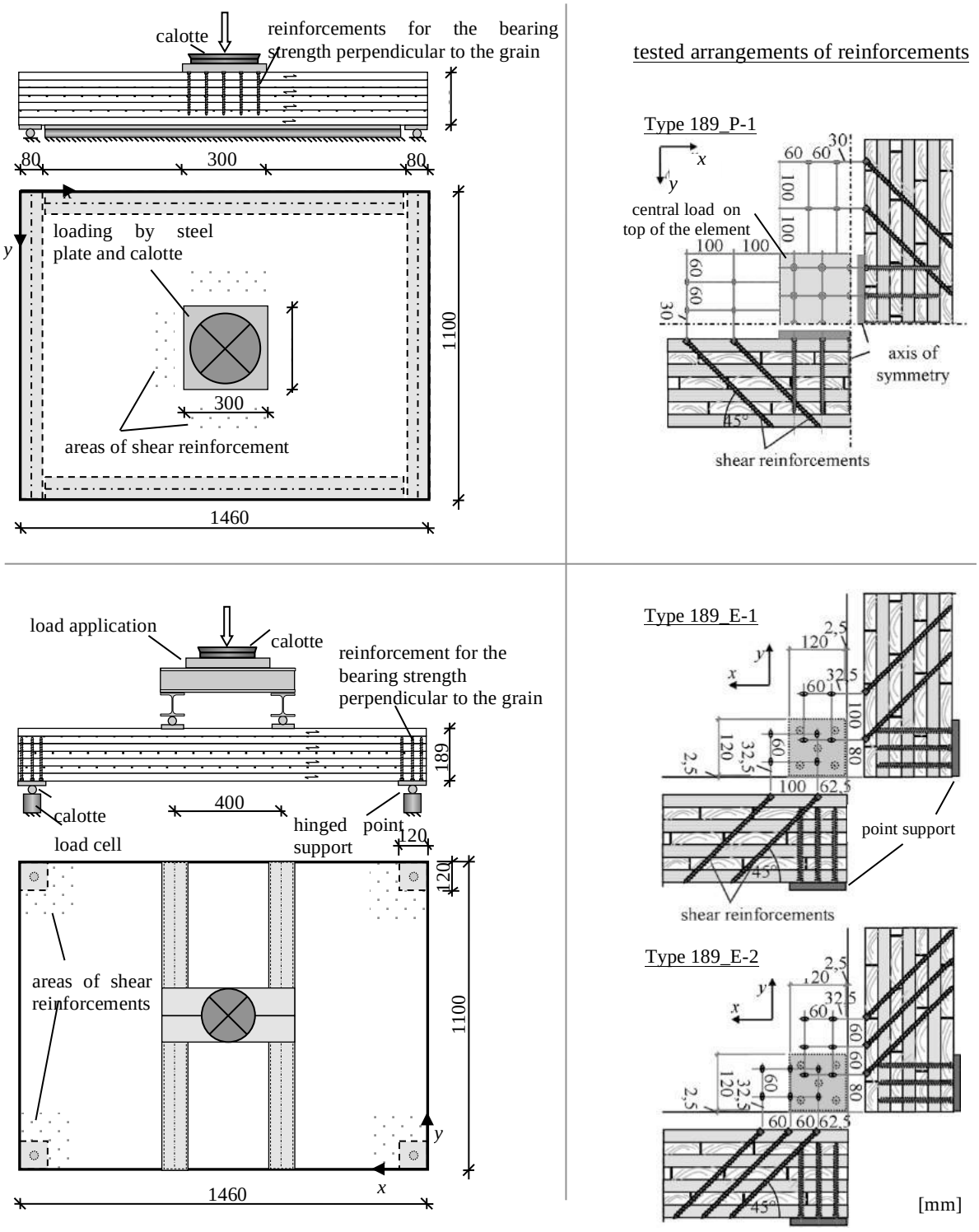

Fig. 10 Test configurations and arrangements of reinforcement

One unreinforced series of each configuration was tested to determine the reference values of the shear capacity. Then the series of reinforced elements shown in Fig. 10 were carried out. The series "Type 189_E-2" consisted of two, all others of three test specimens. Table 6 shows the strengthening factors $\eta_{mean,i}$ calculated by means of the proof loads according to equation (1)

analogous to the tests on beam elements. The increase in load-carrying capacity ranged between 26 % and 49 %.

Tab. 6 Mean values of proof loads and strengthening factor ηmean,i

test configuration	central load Type 189_P-i		point support in corner region Type 189_E-i		
series i =	0 (unreinforced)	1 (reinforced)	0 (unreinforced)	1 (reinforced)	2 (reinforced)
mean value of proof loads $F_{mean,i}$ [kN]	381,1	479,4	304,9	409,7	455,6
COV [-]	0,05	0,02	0,04	0,05	0,01
strengthening factor $\eta_{mean,i}$ [-]	-	**1,26**	-	**1,34**	**1,49**

Due to the biaxial load transfer it is not possible to analytically calculate the rolling shear capacity by means of the proof loads. FEM-simulations were necessary to evaluate the rolling shear stresses at the time of failure. The simulations were done with the program ANSYS [13] using a solid model taking into account the symmetrical conditions (Fig. 11). The rolling shear stresses determined by the simulations exceed the rolling shear capacity according to the four-point-bending tests by up to 70 %. Further examinations revealed that this cannot be explained only by the stress interaction. Hence it may be assumed, that in case of biaxial load transfer additional effects like dispersion and redistribution of stresses or dowelling effects caused by less stressed areas get activated and thus lead to these comparatively high strength values.

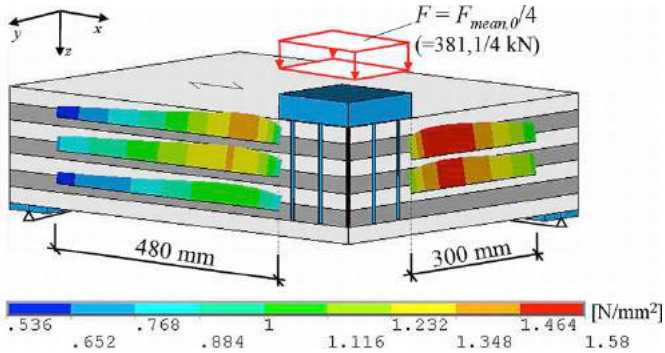

Fig. 11 Distribution of rolling shear stresses of the series "Type 189_P-0" (unreinforced element)

3. Calculation of internal forces and stresses

In contrast to simply supported CLT slabs with uniformly distributed loads there are no calculation toolkits or design charts for constructions with point supports or concentrated loads available that guarantee a cost-effective and safe design. In the case of shear-design it is first of all necessary to evaluate the distribution of shear forces in primary and secondary supporting direction to be able to calculate the critical shear stresses. Hence different influencing factors concerning the distribution of shear forces were examined by means of a parametric study in order to find an approach for the simple estimation of shear stressing. The calculations of this study were carried out using girder-grid-models in order to avoid stress peaks caused by concentrated loads and to minimize the computational effort. The required stiffnesses were calculated according to annex D.3 of the German design code DIN 1052 [2] using the material constants of boards of the strength class C 24.

Different influencing variables concerning the distribution of shear forces were evaluated. Detailed descriptions can be found in [3] and [4]. The significant variables and considered limits were:

- Thickness d of the elements: $0{,}10\ \text{m} < d < 0{,}22\ \text{m}$
- Ratio of the spans l/b: $1 < l/b < 3$
- Number of layers n: $5 < n < 11$
- Square support (Fig. 13/14) $b_{A,x} = b_{A,y}$

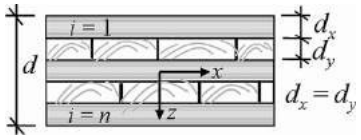

Fig. 12 Examined section type

The following structural systems were analysed:

- Central point support respectively concentrated loading
- Point support in the corner region

The results reveal that in the analysed systems the distribution of shear forces is predominantly influenced by the number of layers. Other parameters, like the ratio l/b of the element dimensions or its thickness can be neglected. So the shear force in the primary direction can be calculated by applying the following equations and the shear force in the secondary direction by the equilibrium of the forces.

- Central point support / concentrated loading (Fig. 13): $V_{xz} \approx 0{,}33 \cdot n^{-0{,}1} \cdot F_k$ (5)
- Point support in the corner region (Fig. 14): $V_{xz} \approx 0{,}67 \cdot n^{-0{,}1} \cdot F_k$ (6)

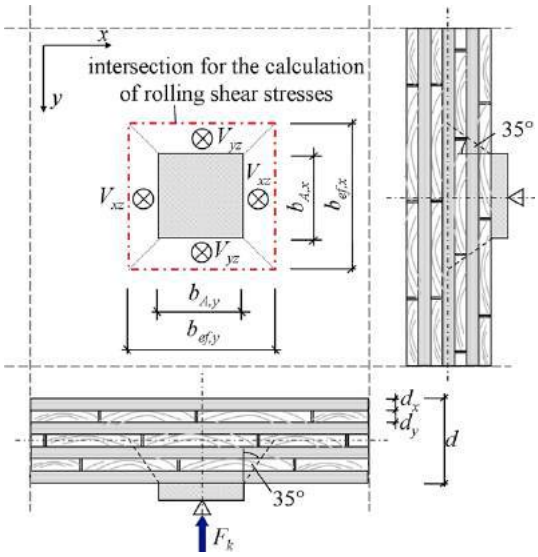

Fig. 13 Central point support / concentr. loading

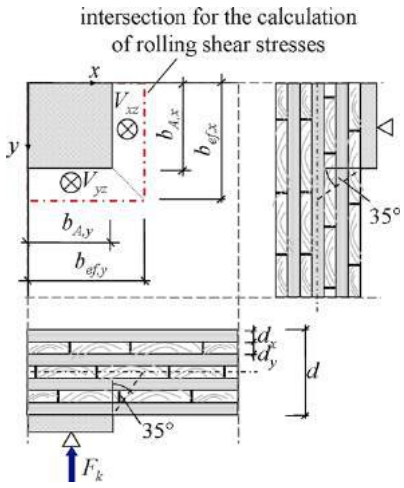

Fig.14 Point support in the corner region

The calculation of the rolling shear stresses along the edges of the support leads to conservative but inefficient results. Hence different approaches of the load distribution were analysed by FEM-simulations using solid models [4]. It appeared that for the analysed systems and conditions the load distribution can be assumed at an angle of 35° to the centre line of the CLT elements. So the governing rolling shear stresses can be calculated by using the effective width shown in Fig. 13 and Fig. 14.

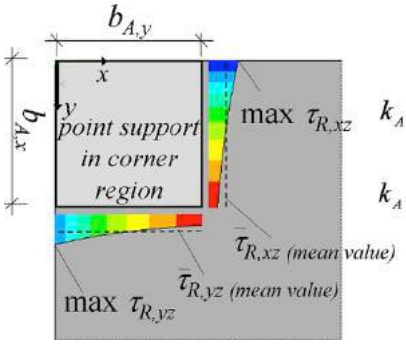

$$k_A = \frac{\max \tau_{R,xz}}{\bar{\tau}_{R,xz}} \quad (7)$$

$$k_A = \frac{\max \tau_{R,yz}}{\bar{\tau}_{R,yz}} \quad (8)$$

Fig. 15 Distribution of stresses

In addition the simulations show that there is a relatively constant distribution of shear stresses along the edges of central point supports. In contrast to this an increase of shear stresses in direction of the edges can be observed along the support edges of point supports in the corner regions (Fig. 15). This increase is according to the calculations in [4] more distinctive with growing ratio of the width of the supports to the thickness of the element. But the analyses of the effective width were based on the assumption that there is a constant distribution of shear stresses. Therefore it was necessary to determine a parameter k_A that considers the increase mentioned. Taking all results into account the rolling shear stresses can be calculated by the following simplified equations:

$$\tau_{R,xz} = \frac{V_{xz} / b_{ef,x}}{k_{R,x} \cdot (d_x + d_y)} \cdot k_A \quad (9)$$

$$\tau_{R,yz} = \frac{V_{yz} / b_{ef,y}}{k_{R,y} \cdot (d_x + d_y)} \cdot k_A \quad (10)$$

Tab. 7 Parameter kR,x and kR,y [-]

number of layers n	5	7	9	11
$k_{R,x}$	2,00	2,50	3,33	3,89
$k_{R,y}$	1,00	2,00	2,50	3,33

Tab. 8 Parameter kA [-]

ratio of $b_{A,x}/d$ or $b_{A,y}/d$		≤ 1,0	≤ 1,5	≤ 2,0
point support in corner region	k_A=	1,35	1,50	1,65
central point support / concentrated loading	k_A=	1,00		

The equations can also be used for beam elements under uniaxial load transfer. In this case the effective width corresponds with the width of the beam and k_A is k_A = 1,0.

Note: In the equations (9) and (10) there is no differentiation of the shear forces of plane A and B according to the shear analogy (annex D.3 of DIN 1052 [2]), because this simplified assumption was taken as the basis within the determination of the effective width.

4. Design concept

The FEM-models described in [3] and [4] on the basis of shell or volume elements are mainly suited for academic research or the analysis of special constructional details. But these simulations are comparatively complex and error-prone because of the great number of input parameters. For a general design concept it makes more sense to use a strut and tie model, which describes the structural behaviour of the composite section of CLT and self-tapping screws in a simplified manner. So it needs considerably fewer input parameters.

The following conditions, for limits of application, were defined to guarantee the verification by the results of the experimental tests and to realize a practical design concept.

- Symmetrical cross section
- Inclination of 45° of the screws
- Arrangements of the screws according to Fig. 16

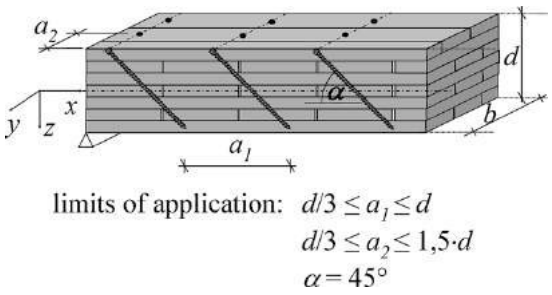

Fig. 16 Arrangements of the screws

4.1 Uniaxial load transfer

According to this design concept the load-carrying capacity under shear stresses of reinforced CLT elements is composed of the rolling shear capacity of the cross layer itself and the proportionate load-carrying capacity of the screws. The assumption of this simultaneous effect is justified, because the experimental tests show that, despite the small shear deformation of the CLT elements, tension forces are activated in the screws. For the calculation of the proportionate load-carrying capacity of the screws, the model shown in Fig 17 can be used. The screws, symbolised by the diagonal struts, bear forces parallel to the shear plane. Due to the fact, that it is mainly a shear model the influence of bending is neglected. The screws in tension additionally cause compression perpendicular to the shear plane which affects the rolling shear capacity positively. In Fig. 17, springs symbolize the transfer of the compression forces. The influence of the stress interaction is considered by the parameter $k_{R,90}$ determined in chapter 2.2.

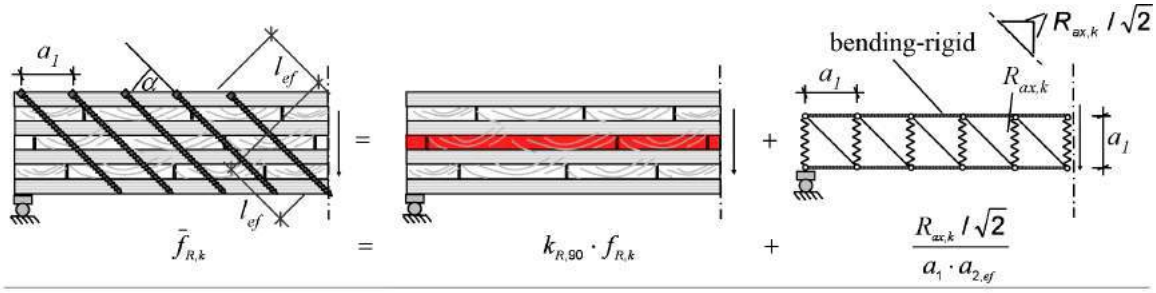

$\bar{f}_{R,k}$	charact. load-carrying capacity of the reinforced CLT under shear stresses	[N/mm²]
$f_{R,k}$	charact. rolling shear capacity (according to technical approvals)	[N/mm²]
$R_{ax,k}$	charact. load-carrying capacity of a screw parallel to its axis	[N]
a_1	distance of the screws parallel to the load bearing direction	[mm]
$a_{2,ef}$	effective distance of the screws perpendicular to the load bearing direction	[mm]
l_{ef}	effective embedment length of the screws for the calculation of $R_{ax,k}$	[mm]
$k_{R,90}$	parameter for the consideration of the stress interaction	[-]

Fig. 17 Design concept on the basis of a strut and tie model

In this case the capacity of the screws is essentially dependent on their withdrawal strength. Universal equations for its calculation are currently not available for an inclination of 45°. However, the investigations within this research project revealed that on the basis of the result of BLAß & UIBEL [14] the withdrawal strength $R_{ax,k}$ of the screws can be calculated approximately according to equation (11).

$$R_{ax,k} = \min\begin{cases} 24{,}8 \cdot d^{0,8} \cdot \ell_{ef}^{0,9} \\ R_{t,u,k} \end{cases} \quad [\text{N}] \tag{11}$$

d diameter of the screws in mm

l_{ef} effective embedment length of the screws in mm

$R_{t,u,k}$ tensile capacity (according to technical approvals)

The effective embedment length l_{ef}, according to equation (12) is dependent on the position of the layer. It results from the minimal penetration length of the screws, based on the centre line of the decisive layer. Fig. 18 shows typical geometric relations.

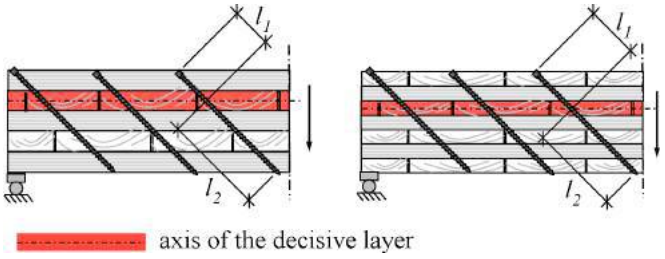

$$l_{ef} = \min\begin{cases} l_1 \\ l_2 \end{cases} \tag{12}$$

Fig. 18 Definition of the effective embedment length l_{ef} of the screws

The compression perpendicular to the grain should be determined by the vertical force component of the screws and the distances between them. Equation (14) delivers the effective distance $a_{2,ef}$, which is the minimum of the real distance a_2 and the quotient of the element width b and the number of screw lines $n_\perp$ perpendicular to the load bearing direction.

$$\sigma_{c,90} = \frac{R_{ax,k} / \sqrt{2}}{a_1 \cdot a_{2,ef}} \qquad \text{with} \quad a_{2,ef} = \max\begin{cases} a_2 \\ b / n_\perp \end{cases} \tag{13) and (14}$$

The influence of the stress interaction should be considered by the parameter $k_{R,90}$:

$$k_{R,90} = \min\begin{cases} 1 + 0{,}35 \cdot \sigma_{c,90} \\ 1{,}20 \end{cases} \quad [-] \qquad \text{with } \sigma_{c,90} \text{ in N/mm}^2 \tag{15}$$

This finally leads to the following shear verification for reinforced CLT according to the design model shown in Fig. 17.

$$\tau_{R,d} \le k_{\text{mod}} \cdot \frac{\bar{f}_{R,k}}{\gamma_M} \qquad \text{with} \quad \bar{f}_{R,k} = k_{R,90} \cdot f_{R,k} + \frac{R_{ax,k} / \sqrt{2}}{a_1 \cdot a_{2,ef}} \tag{16) and (17}$$

4.2 Biaxial load transfer

Even unreinforced CLT elements show high compressive stresses perpendicular to the grain in areas of point supports or concentrated loading. So the positive influence of the stress interaction on the rolling shear capacity should be considered in the shear design of CLT elements without reinforcement. The compression $\sigma_{c,90}$ perpendicular to the grain and the governing rolling shear stress $\tau_{R,d}$ have to be determined by capable computation programs. In standard cases the stresses can also be estimated by the effective width $b_{ef,x}$ and $b_{ef,y}$, which result from the load distribution at an angle of 35° to the centre line of the elements (Fig. 19 and Fig. 20).

$$\sigma_{c,90} = \frac{F_k}{b_{ef,x} \cdot b_{ef,y}} \qquad \text{with} \quad F_k\text{: charact. support force or concentrated load} \tag{18}$$

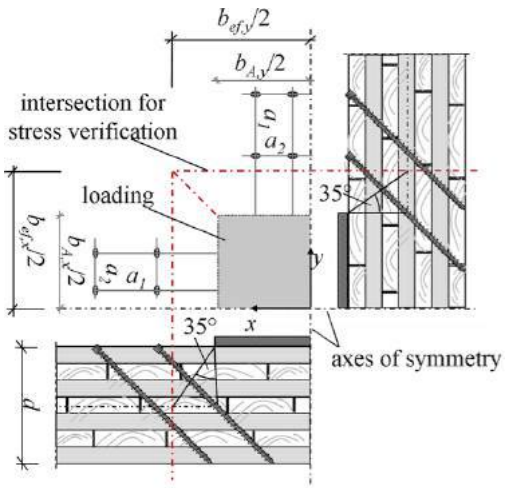

Fig. 19 Central point support / concentr. loading

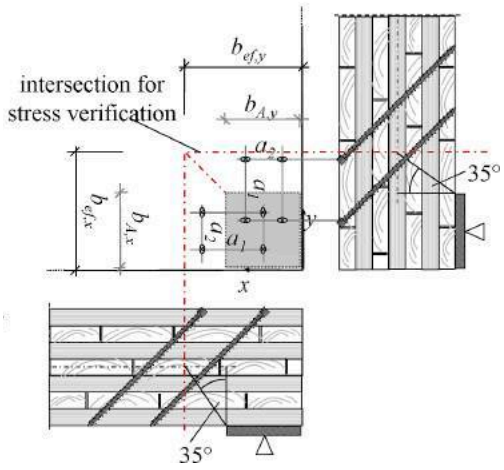

Fig. 20 Point support in the corner region

Again in the course of the stress verification the influence of the stress interaction ought to be considered by the parameter $k_{R,90}$ according to equation (15):

$$\tau_{R,d} \le k_{\text{mod}} \cdot \frac{k_{R,90} \cdot f_{R,k}}{\gamma_M} \tag{19}$$

The design concept for reinforced CLT elements under biaxial load transfer is also generally based on the strut and tie model for beam elements shown in Fig. 17. However, in this case there is no clearly definable element width. So instead of the beam width b the effective width $b_{ef,x}$ or $b_{ef,y}$ has to be used to determine the effective distance of the screw lines $a_{2,ef}$ perpendicular to the load bearing direction. In primary direction $a_{2,ef}$ is:

$$a_{2,ef} = \max \begin{cases} a_2 \\ b_{ef,x} / n_{\perp} \end{cases} \tag{20}$$

with $n_{\perp}$: number of screw lines $n_{\perp}$ perpendicular to the load bearing direction

The total compression $\sigma_{c,90}$ perpendicular to the grain, needed for the determination of the parameter $k_{R,90}$, is the result of the superposition of the compression components caused by the concentrated loading and vertical force component of the screws:

$$\sigma_{c,90} = \frac{F_k}{b_{ef,x} \cdot b_{ef,y}} + \frac{R_{ax,k} / \sqrt{2}}{a_1 \cdot a_{2,ef}} \tag{21}$$

In the course of the shear verification in equation (22) the shear stress $\tau_{R,d}$, determined on the basis of an unreinforced cross section, has to be compared with the load-carrying capacity of the reinforced elements according to the strut and tie model. Again the rolling shear stresses have to be calculated by capable computation programs or can be estimated by the simplified method using an effective width as described in chapter 3.

$$\tau_{R,d} \le k_{\text{mod}} \cdot \frac{\bar{f}_{R,k}}{\gamma_M} \qquad \text{with} \qquad \bar{f}_{R,k} = k_{R,90} \cdot f_{R,k} + \frac{R_{ax,k} / \sqrt{2}}{a_1 \cdot a_{2,ef}} \tag{22) and (23}$$

4.3 Verification of the design concept

In order to verify the proposal of the design concept the charts in Fig. 21 contain the characteristic load-carrying capacity according to the strut and tie model as well as the proof loads, the mean values and the 5%-quantile values of the four-point-bending test.

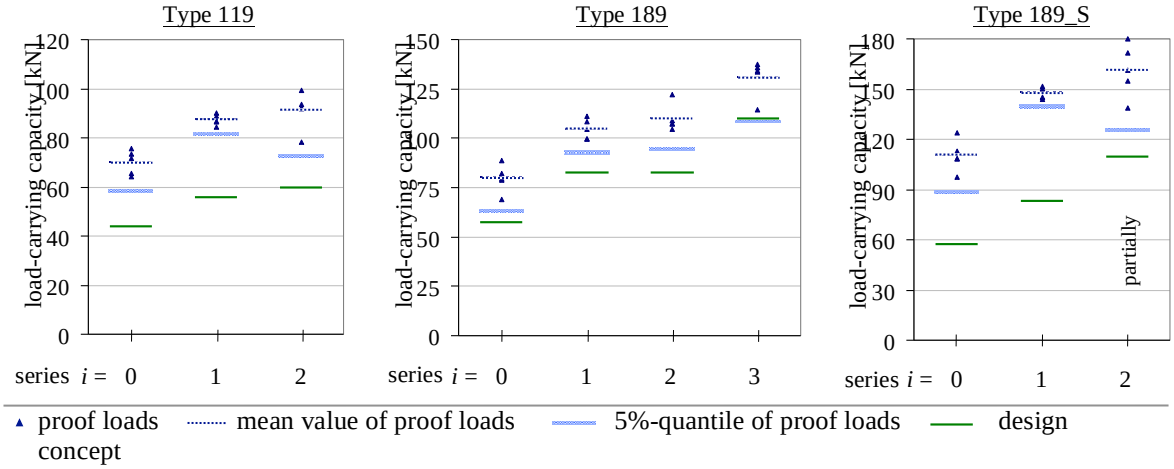

Fig. 21 Comparison of the test results (four-point-bending test) with the design concept

The charts in Fig. 22 show the analogical comparison of the design concept with the results of tests on biaxial load transfer. This time the design concept delivers two components of the load-carrying capacity. Hence the values $F_{max,x,i}$ and $F_{max,y,i}$ indicate the load-carrying capacity according to the strut and tie model in primary and secondary direction. The stresses were calculated according to the simplified method described in chapter 3.

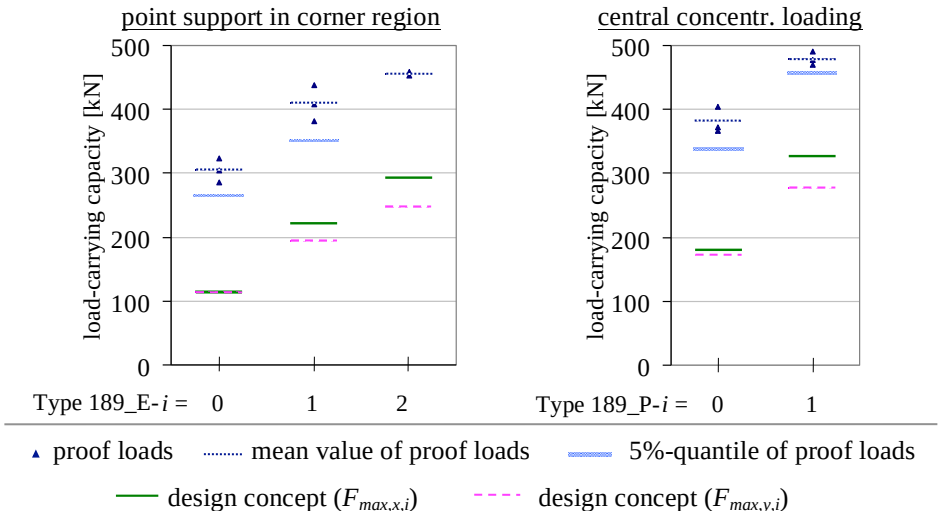

Fig. 22 Comparison of the test results with the design concept – biaxial load transfer

The comparisons verify that the proposed design model represents a conservative approach for the shear design of reinforced CLT. The difference between the values of the design concept and the mean values remains quite constant for each element type. This signifies that the increase in load-carrying capacity, as a result of the reinforcement, is covered fairly well by the design concept. But, especially under biaxial load transfer, the base level, which means the design value of the unreinforced series, is considerably underestimated. This corresponds to the results of the FEM-simulations, which also delivered, for the unreinforced series, considerably higher rolling

shear stresses than the rolling shear capacity determined by tests on beam elements under uniaxial load transfer.

5. Conclusion

The results presented in this paper allow the shear design of CLT under concentrated loading, considering reinforcement by inclined self-tapping screws with continuous threads. The main conclusions delivered by the described research project are:

- Concentrated loading in CLT elements causes a combination of high shear stresses and compression perpendicular to the grain. By means of experimental tests, the positive effect of this stress interaction on the rolling shear capacity was verified and a design concept is proposed.
- Self-tapping screws with continuous threads are a simple and efficient reinforcement. They allow a cost-effective shear design of CLT structures, as they can be applied systematically in localised areas with high shear stresses. Thus they increase the load-carrying capacity in the decisive areas. A simplified design concept validated by means of test results is recommended. It is based upon a strut and tie model and can be used for beam elements as well as plate elements under concentrated loading.
- In the case of a biaxial load transfer, additional effects are activated, leading to an increase in the rolling shear capacity compared to that of beam elements. For economic reasons it should be analysed how far the redundant structural behaviour may be considered for the shear verification. One approach might be the use of increased values for the rolling shear capacity in cases of biaxial load transfer.

6. Acknowledgement

The research project was kindly supported by the German Society of Wood Research (DGfH) and the International Association for Technical Issues related to Wood (iVTH). Special gratitude is extended to the German Federation of Industrial Research Associations (AiF) for funding the project with financial means of the German Federal Ministry of Economics and Technology (BMWi).

7. Literature

[1] Mestek, P.; Winter, S.: Design Concept for CLT - reinforced with Self-Tapping Screws. International Council for Research and Innovation in Building and Construction - Working Commission W18 - Timber Structure (CIB-W18); Alghero, Italy, 08/2011.

[2] DIN 1052:2008-12: Entwurf, Berechnung und Bemessung von Holzbauwerken. Allgemeine Bemessungsregeln und Bemessungsregeln für den Hochbau.

[3] Mestek, P.; Winter, S.: Konzentrierte Lasteinleitung in Brettsperrholzkonstruktionen - Verstärkungsmaßnahmen. Schlussbericht zum AiF-Forschungsvorhaben Nr. 15892, TU München, 2011.

[4] Mestek, P: Punktgestützte Flächentragwerke aus Brettsperrholz (BSP) - Schubbemessung unter Berücksichtigung von Schubverstärkungen. Dissertation, TU München, 10/2011.

[5] Colling, F.; Bedö, S.: Prüfbericht Nr.: H06-01/1-ZE-PB; Kompetenzzentrum Konstruktiver Ingenieurbau, Abteilung Holzbau, Fachhochschule Augsburg, unpublished, 2007.

[6] DIN 4074-1:2008-12: Sortierung von Holz nach der Tragfähigkeit – Teil 1: Nadelschnittholz.

[7] Spengler, R.: Festigkeitsverhalten von Brettschichtholz unter zweiachsiger Beanspruchung, Teil 1 - Ermittlung des Festigkeitsverhaltens von Brettelementen aus Fichte durch Versuche. Hrsg.: Laboratorium für den Konstruktiven Ingenieurbau (LKI), Berichte zur Zuverlässigkeitstheorie der Bauwerke H.62/1982.

[8] Hemmer, K.: Versagensarten des Holzes der Weißtanne (Abies Alba) unter mehrachsiger Beanspruchung. Dissertation, TH Karlsruhe, 1984.

[9] Sofistik 2010 Statik. Sofistik AG, Oberschleißheim, 2009.

[10] Common Understanding of Assessment Procedure: “Solid wood slab element to be used as a structural element in buildings”; ETA request No 03.04/06, Austria, 2005.

[11] abZ. Nr. Z-9.1-519 vom 07. Mai 2007; SPAX-S Schrauben mit Vollgewinde als Holzverbindungsmittel; ABC Verbindungstechnik GmbH & Co. KG, Ennepetal, Deutschland; Deutsches Institut für Bautechnik, Berlin, 2007.

[12] Bejtka, I.: Verstärkungen von Bauteilen aus Holz mit Vollgewindeschrauben. Dissertation erschienen in: Karlsruher Berichte zum Ingenieurholzbau 2, Universitätsverlag Karlsruhe, 2005.

[13] ANSYS, Finite Elemente Programm, Release 12.0.

[14] Blaß, H.J.; Uibel, T.: Bemessungsvorschläge für Verbindungsmittel in Brettsperrholz. Bauen mit Holz, Heft 2, 2009.